Gas-Sorption Properties of Cobalt(II)–Carborane-Based Coordination Polymers as a Function of Morphology**

Omar K. Farha, Alexander M. Spokoyny, Karen L. Mulfort, Simona Galli, Joseph T. Hupp, and Chad A. Mirkin**

Coordination-polymer materials represent a rapidly growing area in modern chemistry and materials science. These structures can now be made in many forms, including crystalline metal–organic frameworks (MOFs)[1] and well-defined (in terms of size and shape) infinite-coordination-polymer (ICP) nano- and microparticles.[2] These materials show promise in many applications, including catalysis,[3] gas storage,[4] separation processes,[5] ion exchange,[6] small-molecule detection,[7] drug delivery,[8] and optoelectronics.[9] The properties of the coordination polymers and, therefore, their potential for application can be highly dependent on bulk and microscopic structure, yet little has been done to compare and contrast one set of structures as a function of morphology and particle size.

Thus far, much more attention has been devoted to the study of crystalline macroscopic MOFs[10] than to other potential morphologies[2a] of coordination-polymer materials. Indeed, only a handful of reports[2j,11–12] involve adsorption studies of amorphous metal–organic microparticles, semicrystalline materials, and nanostructures. Interestingly however, none of these studies address how the gas-sorption properties of one class of coordination polymer depend on morphology.[12] Understanding the differences in the gas-uptake properties of materials with nearly identical chemical compositions and similar metal-coordination environments but different morphologies could provide insight into how one can optimize a particle composition with respect to gas uptake (both rate and capacity) and selectivity.

We recently reported a crystalline Zn^{II} carborane[13] based MOF (CB-MOF-1),[4b] which was synthesized from 1,12-dihydroxycarbonyl-1,12-dicarba-*closo*-dodecaborane (**1**) (p-$CDCH_2$). Compound **1** and cobalt(II) salts were used successfully to synthesize three new coordination-polymer materials simply by varying the reaction solvent and temperature conditions. All of them have different morphologies, defined in part by different degrees of crystallinity — two crystalline MOFs, isolated as blocklike single crystals **2** or polycrystalline tetragonal microrods **3**, and a less-crystalline material in the form of agglomerates **4** (Figure 1).

The solvothermal reaction between **1** and cobalt nitrate hexahydrate $Co(NO_3)_2 \cdot 6H_2O$ at 90 °C in DMF/EtOH (1:1) over 24 h led to the new crystalline MOF $[Co_4(OH)_2(p\text{-}CDC)_3DMF_2]_n$ (**2**) in 70% yield (based on **1**). Compound **2** was characterized by elemental analysis, TGA, FTIR, and single-crystal X-ray diffraction studies (see Supporting Information). The structure[14] of **2** consists of a node with four Co^{II} atoms bridged by two μ^3 hydroxy groups and contains two η^1-DMF molecules at each Co^{II} center. These clusters are held together through neighboring Co^{II} atoms sharing one carboxylate from p-CDC^{2-}, which is bound in an η^2 fashion.

The microcrystalline rods $[Co(p\text{-}CDC)(pyridine)_2(H_2O)]_n$ (**3**) were prepared in 77% yield by heating a mixture of **1** and $Co(OAc)_2 \cdot 4H_2O$ (1:1 molar ratio) in 1-butanol/water/pyridine at 95 °C for 2.5 h. This material was characterized by scanning electron microscopy (SEM), energy-dispersive X-ray spectroscopy (EDS), elemental analysis, thermogravimetric analysis (TGA), and Fourier-transform Infrared spectroscopy (FTIR). Moreover, we used X-ray powder diffraction (XRPD) methods to determine its crystal and molecular structure (see Supporting Information and Figure 2).[14] The structure consists of Co^{II} nodes in which the metal ions exhibit *cis*-N_2O_4 octahedral stereochemistry. The coordination environment of each Co^{II} consists of four ligated oxygen atoms derived from three carboxylate groups of three different p-CDC ligands. One of these carboxylates is bound in an η^1-fashion to a single metal center, and the others are bound in a bridging fashion to two different Co^{II} atoms.

---

[*] Prof. J. T. Hupp, Prof. C. A. Mirkin, Dr. O. K. Farha, A. M. Spokoyny, K. L. Mulfort
Department of Chemistry and the International Institute for Nanotechnology
Northwestern University
2145 Sheridan Road, Evanston, IL 60208-3113 (USA)
E-mail: chadnano@northwestern.edu; j-hupp@northwestern.edu
Dr. S. Galli
Dipartimento di Scienze Chimiche e Ambientali
Universitá degli Studi dell'Insubria
Via Valleggio, 11 22100 Como (Italy)

[**] O.K.F. and A.M.S. contributed equally to this work. C.A.M. acknowledges the ARO, AFOSR, ONR, and NSF for supporting this work. J.T.H. acknowledges the Northwestern University Nanoscale Science and Engineering Center (NSEC) (DOE grant DE-FG02-08ER-15967) and Argonne Natl. Lab (Lab-Grad Fellowship for K.L.M.) for financial support. The authors are grateful to Tina Li for help with SEM. S.G. thanks the Fondazione Cariplo for funding (Progetto Cariplo 2007-5117).

Supporting information for this article is available on the WWW under http://www.small-journal.com or from the author.

DOI: 10.1002/smll.200900085

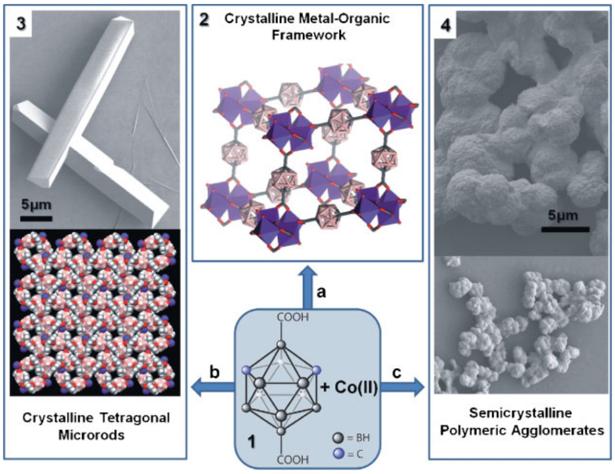

Figure 1. Synthetic scheme for: a) $[Co_4(OH)_2(p\text{-}CDC)_3DMF_2]_n$ (**2**), crystal structure with coordinated solvents omitted for clarity; b) $[Co(p\text{-}CDC)(pyridine)_2(H_2O)]_n$ rods (**3**), and c) agglomerates **4**.

The remaining two sites are occupied by η^1-bound pyridine moieties. The coordination modes of the *p*-CDC ligand generate two distinct structural motifs, namely four- and eight-membered rings, which reciprocally organize to yield two, interpenetrated, polymeric networks. The channels in **3** are aligned along the crystallographic *c* axis. They are filled with water molecules and decorated with the pyridine moieties, which are coordinated to the Co^{II} centers.

The agglomerates **4** were synthesized in 69% yield by overnight diffusion of diethyl ether into a solution of **1** and $Co(OAc)_2 \cdot 4H_2O$ (1:1 molar ratio) in DMF. This approach is similar to that used to prepare conventional coordination-polymer particles.[2a] The agglomerates were characterized by the same techniques used to characterize **3**, and all data suggest that **2**–**4** have the same basic connectivity with different amounts of solvent and types of ancillary ligands coordinated to the Co nodes (DMF or pyridine).

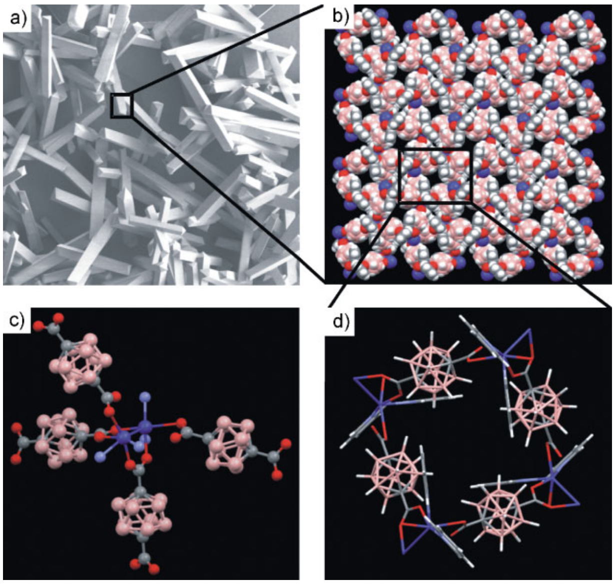

Figure 2. a) SEM image of **3**, b) space-filling model of the extended network without water/pyridine molecules, c) connectivity of Co^{II}–Co^{II} secondary building unit cluster (pyridine carbon backbones are omitted for clarity), and d) a channel within the 3D network.

SEM images of the as-synthesized substances reveal distinct differences in morphology. The agglomerates appear as disordered 5–10-μm fused semispherical units with rough surfaces. In contrast, the rods are dome-terminated tetragonal prisms with smooth faces. They can be as long as ≈25 μm (see Supporting Information) and ≈3 μm wide, thus requiring powder and not single-crystal diffraction for their structural characterization. On the macroscopic scale, **2** can be characterized as a series of much larger blocklike crystals. Most importantly, all three materials retain their apparent morphology upon thermally induced solvent desorption.

We have evaluated the stability of the three compounds by TGA (see Supporting Information). All exhibited relatively high stability, showing no sign of framework decomposition until ≈400 °C. The agglomerates **4** begin to lose solvent at 110 °C. In the case of the rods **3**, two major weight-loss steps were observed. One at 120–130 °C is assigned to the liberation of water from the 1D channels and one of the two coordinated pyridine moieties; the second, at ≈250 °C, is assigned to the loss of the remaining coordinated pyridine.[2j] The thermal behavior of species **3** has been further characterized by in situ variable-temperature X-ray diffraction (TXRPD, see Supporting Information). The experiments, carried out in the 30–170 °C range, show an irreversible substantial change in the unit cell parameters at 130 °C. Notably, the tetragonal symmetry is preserved, despite an 18% shrinkage of the unit-cell volume. This transition correlates well with the first mass loss observed in the TGA. Compound **2** also exhibits two thermally induced mass changes, one at ≈100 °C assigned to the loss of pore-filling solvent molecules and one at ≈200 °C assigned to the loss of coordinated DMF. The remarkable thermal stability of the frameworks **2**–**4** can be explained, in part, by the high thermal stability of **1** and is consistent with previous work on carborane organic polymers[13a] and metal-based oligomers[13b] as well as CB-MOF-1.[4b]

All three morphologies have been studied by XRPD (Figure 3). As expected, MOF **2** displays a strong diffraction pattern, characteristic of a highly crystalline material. Its phase purity was confirmed by comparison to the simulated XRPD pattern, generated from the single-crystal data (see Supporting Information). The rods **3** are also quite crystalline and phase-pure. The agglomerates **4** exhibit a diffraction pattern of modest quality, in contrast to **2** and **3**. In light of this experimental data, the agglomerates can be classified as semicrystalline materials.

Nitrogen (N_2) and carbon dioxide (CO_2) adsorption studies (Figure 4 and Supporting Information) of the three materials were performed to probe their porosity. MOF **2**, after being placed under vacuum (for evacuation details see Experimental Section) for 12 h at 250 °C, exhibited a N_2 Brunauer, Emmett, and Teller (BET) surface area of 1080 $m^2\ g^{-1}$. The N_2 BET areas for similarly activated **3** and agglomerates were 351 and 20 $m^2\ g^{-1}$, respectively. Essentially, the agglomerates show no significant N_2 uptake.

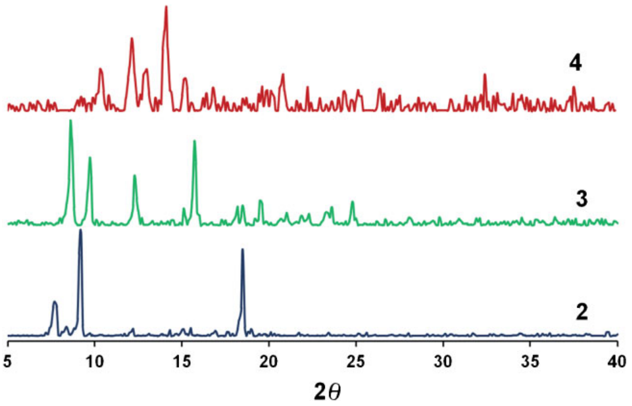

Figure 3. XRPD spectra of bulk MOF **2** (bottom), rods **3** (middle), and agglomerates **4** (top).

Table 1. Summary of carborane-Co^{II} coordination-polymer materials parameters obtained based on N_2-, CO_2-, and H_2-adsorption measurements

Material	Surface area[a]/[b]	Hydrogen uptake[c]	Pore volume[d]	Pore size distribution[e]
2	1080/1150	181	0.42	4.9
3	351/350	75	0.14	5.0
4	20/240	70	0.01	6.3, 8.8

[a] N_2 BET surface area [$m^2\ g^{-1}$] determined in relative pressure range $0.01 < P/P_o < 0.05$.
[b] CO_2 surface area [$m^2\ g^{-1}$] calculated by NLDFT.
[c] $cm^3\ g^{-1}$ at 77 K and 1 atm.
[d] [$cm^3\ g^{-1}$] Saito–Foley method from N_2 isotherm.
[e] Å, obtained by Horwath–Kawazoe method from N_2 isotherm.

Interestingly, the accessible surface area for the agglomerates **4** is highly probe-molecule dependent (Table 1). With CO_2 and the nonlocal density functional theory (NLDFT) method of analysis (see Supporting Information for CO_2 isotherms), the surface area of the agglomerates is 240 $m^2\ g^{-1}$. In contrast, the crystalline materials **2** and **3** yield very similar N_2- and CO_2-derived surface areas. One explanation for this observation may be the slightly smaller kinetic diameter for CO_2 relative to N_2.[2j] It may be that the pores in the agglomerates (or their surface entrances) in **4** are small enough to discriminate between the two gas molecules, whereas the pores in **2** and **3** are too large to discriminate effectively.

Alternatively, the discrimination between N_2 and CO_2 by agglomerates **4** may reflect the temperature difference in the two surface-area-measurement experiments (77 K vs. 273 K), rather than the slight probe-size difference. The higher temperature in the CO_2 experiment will clearly impart greater kinetic energy to the probe molecule as well as facilitate distortion of pores that may otherwise be too narrow to allow probe molecules to enter.[15b]

Pore-size distributions, which were obtained from analysis of the low-pressure region of the N_2 isotherms, are summarized in Table 1. Both **2** and **3** feature very well-defined pores that are ≈5 Å in diameter, whereas the agglomerates **4** show two broad distributions of pore diameters, centered around 6.3 and 8.8 Å. Notably, **2** and **3** exhibit type I isotherms, which are characteristic of microporous materials.[15]

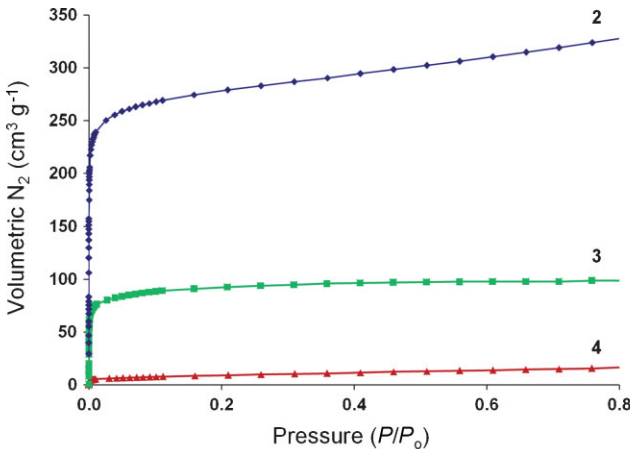

Figure 4. Nitrogen adsorption isotherms for agglomerates **4** (red triangles), rods **3** (green squares), and bulk MOF **2** (blue rhombuses).

The hydrogen-uptake properties of all the materials were also measured, following treatment with heat and vacuum, Figure 5. Whereas **2** has H_2-uptake properties comparable to the crystalline MOF materials, optimized for H_2,[10c] rods **3** and agglomerates **4** exhibit markedly lower but similar H_2-uptake properties. The pores of the agglomerate can accommodate H_2 and CO_2 but not the larger kinetic diameter N_2 (at least at 77 K). Interestingly, the rods, which have a greater N_2-accessible surface area, still do not significantly outperform the agglomerates in H_2 uptake (both ≈75 $cm^3\ g^{-1}$). The observation that all three materials exhibit sufficient porosity to sorb H_2 likely reflects both the small size of the sorbate and the fact that at 77 K, H_2 is well above its critical point (32 K, 1.3 MPa).

Consequently, pore blockage based on aggregation of sorbate molecules at framework bottlenecks is not possible for H_2; on the other hand, bottleneck condensation of N_2 is, in principle, possible. Recent computational studies by Frost et al.[15c] show that at modest pressures, sorption of H_2 by crystalline coordination polymers generally scales with the internal surface area (and at higher pressures, with the pore volume). From Table 1, the extent of H_2 uptake by the three new materials correlates only crudely with internal surface area. Several factors, such as pore volume, pore-wall modification, and diameter of the pore entrance must be taken into consideration. We suggest that an important additional, but related, factor is crystallinity. All else being equal, a material containing highly regular (i.e, efficiently arranged) micropores should offer greater internal surface area per unit mass than one featuring an irregular configuration of micropores. The much larger N_2- and CO_2-accessible surface areas for crystalline **2** and **3** versus the less-crystalline **4** support this notion. At the same time, a material such as **4** should contain a much broader range of pore sizes than an analogous crystalline material.

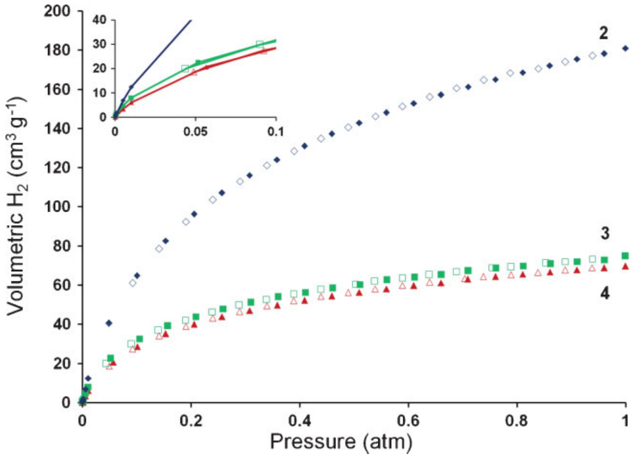

Figure 5. Hydrogen isotherm adsorption (solid) and desorption (empty) for agglomerates **4** (red triangles), rods **3** (green squares), and bulk MOF **2** (blue rhombuses).

From these observations, one can conclude that "good" hydrogen physisorption, at modest pressures, by a coordination polymer requires a combination of crystallinity, permanent microporosity, and sizable internal surface area. Therefore, reducing or eliminating one of these structural features, observed through a change in morphology, may lead to significant changes in adsorbate selectivity and extent of uptake. Indeed, discrimination between N_2 and H_2 is clearly observed in the agglomerates, which exhibit much higher uptake of H_2 than of N_2. Interestingly, the morphologies and porosities of **2** and **3**, and presumably **4**, are strongly coupled with their molecular structures. The solvents DMF, H_2O, and pyridine act as ancillary ligands that significantly affect the type of framework that is formed.[16] Indeed, although they are ultimately removed prior to gas-sorption measurements, the solvent molecules are responsible, in large part, for templating the formation of the different porous structures observed (Figures 1 and 2). On the other hand, if one considers gas discrimination, nonclassical MOF materials (ICPs[2k]) **3** and **4** can be potentially exploited advantageously owing to their variable pore sizes and corresponding apertures as well as ultramicropores.

In conclusion, we have used the same metal ion and organic ligand, but different reaction conditions and cosolvents, to synthesize three morphologically different coordination polymer materials. The three compounds, upon thermal activation, display markedly different capacities and selectivities toward H_2, CO_2, and N_2. These differences can be attributed to the structural differences between the materials, which significantly influence their porosities, crystallinity, and internal surface areas, and as a result, their adsorption capabilities.

Experimental Section

*Synthesis of **2** (Bulk MOF):* A solution of cobalt(II) nitrate hexahydrate ($Co(NO_3)_2 \cdot 6H_2O$) (100 mg, 0.29 mmol) and *p*-$CDCH_2$ (25 mg, 0.12 mmol) were dissolved in DMF/ethanol (1:1, 2.5 mL) in a glass vial and then allowed to react at 90 °C for 24 h. MOF **2** was collected and washed with DMF in 70% yield (based on ligand **1**). For gas-sorption studies, a sample was evacuated at 250 °C for 12 h under dynamic vacuum at 10^{-5} Torr. TGA of the heat-activated sample showed no solvent loss (except water). CHN analysis of the activated sample confirmed significant loss (>90%) of nitrogen from the as-synthesized sample, corresponding to the removal of DMF. Data for the as-synthesized sample **2**: IR (neat): 685 (w), 771 (w), 674 (w), 737 (w), 783 (w), 845 (w), 1114 (w), 1150 (w), 1370 (s, br), 1640 (s, br), 2620 cm^{-1} (m, br); elemental analysis (as-synthesized sample): calcd for $C_{12}H_{32}B_{30}Co_4O_{14} \cdot 4DMF \cdot H_2O$: C 22.68, H 4.92, N 4.41; found: C 22.21, H 5.06, N 4.56.

*Synthesis of **3** (Rods):* Solutions of cobalt(II) acetate tetrahydrate ($Co(OAc)_2 \cdot 4H_2O$) (50 mg, 0.2 mmol) in deionized water (2 mL) and *p*-$CDCH_2$ (47 mg) in *n*-butanol (10 mL) were combined in a glass vial. The reaction vial was heated for 1.5 h in an oven at 95 °C. Pyridine (0.5 mL) was added to the reaction solution while hot, and the mixture was heated in an oven for another 1 h at 90 °C, during which a precipitate formed. The solid was collected and washed twice with methanol and recollected by centrifugation. The product was subsequently dried under vacuum at ambient temperature to afford **3** as a pink solid (55 mg; 77% based on **1**). For gas-sorption studies, a sample was evacuated at 300 °C for 12 h under dynamic vacuum at 10^{-5} Torr. TGA of the heat-activated sample showed no solvent loss (except water). CHN analysis of the activated sample confirmed significant loss (>90%) of nitrogen content from the as-synthesized sample (removal of pyridine). Data for the as-synthesized sample **3**: IR (neat): 698 (w), 737 (w), 778 (w), 1043 (w), 1071 (w), 1220 (w), 1375 (s, br), 1672 (s), 2610 (s, br), 2883 (w), 2940 (w), 2970 cm^{-1} (weak); elemental analysis (as-synthesized sample): calcd for $C_4H_{10}B_{10}CoO_4 \cdot 2pyridine \cdot 1H_2O$: C 36.13, H 4.76, N 6.02; found: C 35.97, H 4.64, N 5.91.

*Synthesis of **4** (Agglomerates):* $Co(OAc)_2 \cdot 4H_2O$ (100 mg, 0.2 mmol) was dissolved in DMF (10 mL) with sonication. The solution was mixed with dissolved *p*-$CDCH_2$ (95 mg, 0.2 mmol) ligand in the same solvent (2 mL). Diethyl ether (3 mL) was layered on top of this solution and allowed to diffuse slowly into the reaction mixture, while stirring the bottom layer at 50 rpm with a magnetic stirrer bar. After 12 h, the agglomerates were collected by centrifugation and washed twice with methanol. The washed particles were dried under vacuum at room temperature to afford **4** (90 mg; 69% based on **1**) as apink powder. For gas sorption, a sample was evacuated at 250 °C for 12 h under dynamic vacuum at 10^{-5} Torr. TGA analysis of the heat-activated sample showed no solvent loss (except water). CHN analysis of the activated sample confirmed significant loss (>90%) of nitrogen from the as-synthesized sample, corresponding to the removal of DMF. Data for the as-synthesized sample **4**: IR (neat): 737 (w), 783 (w), 852 (w), 1021 (m), 1132 (m), 1385 (s, br), 1602 (s), 1661 (m), 2620 cm^{-1} (s, br); elemental analysis (as-synthesized sample): calcd for $C_{12}H_{32}B_{30}Co_4O_{14} \cdot 2DMF \cdot 2H_2O$: C 18.92, H 4.41, N 2.45; found: C 19.20, H 4.47, N 2.89.

Keywords:
carboranes · gas separation · hydrogen storage · infinite coordination polymers · nanoporous materials

---

[1] a) S. L. James, *Chem. Soc. Rev.* **2003**, *32*, 276; b) S. Kitagawa, R. Kitaura, S. Noro, *Angew. Chem. Int. Ed.* **2004**, *43*, 2334; c) G. Ferey, *Chem. Soc. Rev.* **2008**, *37*, 191.

[2] a) M. Oh, C. A. Mirkin, *Nature* **2005**, *438*, 651; b) M. Oh, C. A. Mirkin, *Angew. Chem. Int. Ed.* **2006**, *45*, 5492; c) Y.-M. Jeon, J. Heo, C. A. Mirkin, *J. Am. Chem. Soc.* **2007**, *129*, 7480; d) H. Maeda, M. Hasegawa, T. Hashimoto, T. Kakimoto, S. Nishio, T. Nakanishi, *J. Am. Chem. Soc.* **2006**, *128*, 10024; e) K. H. Park, K. Jang, S. U. Son, D. A. Sweigart, *J. Am. Chem. Soc.* **2006**, *128*, 8740; f) X. Sun, S. Dong, E. Wang, *J. Am. Chem. Soc.* **2005**, *127*, 13102; g) H. Wei, B. Li, Y. Du, S. Dong, E. Wang, *Chem. Mater.* **2007**, *19*, 2987; h) S. Jung, M. Oh, *Angew. Chem. Int. Ed.* **2008**, *120*, 2079; i) W. J. Rieter, K. M. L. Taylor, H. An, W. Lin, W. Lin, *J. Am. Chem. Soc.* **2006**, *128*, 9024; j) Y.-M. Jeon, G. S. Armatas, J. Heo, M. G. Kanatzidis, C. A. Mirkin, *Adv. Mater.* **2008**, *20*, 2105; k) A. M. Spokoyny, D. Kim, A. Sumrein, C. A. Mirkin, *Chem. Soc. Rev.* **2009**, in press; l) Y.-M. Jeon, G. S. Armatas, D. Kim, M. G. Kanatzidis, C. A. Mirkin, *Small* **2009**, *5*, 46.

[3] a) S.-H. Cho, B. Ma, S. T. Nguyen, J. T. Hupp, T. E. Albrecht-Schmitt, *Chem. Commun.* **2006**, 2563; b) J. S. Seo, D. Wand, H. Lee, S. I. Jun, J. Oh, Y. Jeon, K. Kim, *Nature* **2000**, *404*, 982; c) T. Sawaki, Y. Aoyama, *J. Am. Chem. Soc.* **1999**, *121*, 4793; d) B. Kesanli, W. Lin, *Coord. Chem. Rev.* **2003**, *246*, 305; e) A. Hu, H. L. Ngo, W. Lin, *J. Am. Chem. Soc.* **2003**, *125*, 11490; f) C.-D. Wu, A. Hu, L. Zhang, W. Lin, *J. Am. Chem. Soc.* **2005**, *127*, 8940; g) M. Fujita, Y.-J. Kwon, S. Washizu, K. Ogura, *J. Am. Chem. Soc.* **1994**, *116*, 1151.

[4] a) K. L. Mulfort, J. T. Hupp, *J. Am. Chem. Soc.* **2007**, *129*, 9604; b) O. K. Farha, A. M. Spokoyny, K. L. Mulfort, M. F. Hawthorne, C. A. Mirkin, J. T. Hupp, *J. Am. Chem. Soc.* **2007**, *129*, 12680; c) M. Dinca, A. Dailly, Y. Liu, C. M. Brown, D. A. Neumann, J. R. Long, *J. Am. Chem. Soc.* **2006**, *128*, 16876; d) H. J. Choi, M. P. Suh, *J. Am. Chem. Soc.* **2004**, *126*, 15844; e) E. Y. Lee, M. P. Suh, *Angew. Chem. Int. Ed.* **2004**, *43*, 2798; f) D. Bradshaw, J. B. Claridge, E. J. Cussen, T. J. Prior, M. J. Rosseinsky, *Acc. Chem. Res.* **2005**, *38*, 273; g) S. Kitagawa, R. Kitaura, S. Noro, *Angew. Chem. Int. Ed.* **2004**, *43*, 2334; h) M. Latroche, S. Surblé, C. Serre, C. Mellot-Draznieks, P. L. Llewellyn, H. Lee, J. Chang, S. H. Jhung, G. Férey, *Angew. Chem. Int. Ed.* **2006**, *45*, 8227; i) E. Welch, J. R. Long, *Angew. Chem. Int. Ed.* **2007**, *46*, 3494; j) Y. Liu, J. F. Eubank, A. J. Cairns, J. Eckert, V. C. Kravtsov, R. Luebke, M. Eddaoudi, *Angew. Chem. Int. Ed.* **2007**, *119*, 3342; k) J. C. Rowsell, O. M. Yaghi, *Angew. Chem. Int. Ed.* **2005**, *44*, 4670; l) K. L. Mulfort, J. T. Hupp, *Inorg. Chem.* **2008**, *47*, 7936.

[5] a) K. S. Min, M. P. Suh, *Chem. Eur. J.* **2001**, *7*, 303; b) K. Uemura, S. Kitagawa, M. Kondo, K. Fukui, R. Kitaura, H.-C. Chang, T. Mizutani, *Chem. Eur. J.* **2002**, *8*, 3586; c) M. P. Suh, J. W. Ko, H. J. Choi, *J. Am. Chem. Soc.* **2002**, *124*, 10976; d) R. Kitaura, K. Seki, G. Akiyama, S. Kitagawa, *Angew. Chem. Int. Ed.* **2003**, *42*, 428; e) R. Q. Snurr, J. T. Hupp, S. T. Nguyen, *AIChE* **2004**, *50*, 1090; f) Y. S. Bae, K. L. Mulfort, H. Frost, P. Ryan, S. Punnathanam, L. J. Broadbelt, J. T. Hupp, R. Q. Snurr, *Langmuir* **2008**, *24*, 8592; g) Y. S. Bae, O. K. Farha, A. M. Spokoyny, C. A. Mirkin, J. T. Hupp, R. Q. Snurr, *Chem. Commun.* **2008**, 4135; h) D. Bradshaw, T. J. Prior, E. J. Cussen, J. B. Claridge, M. J. Rosseinsky, *J. Am. Chem. Soc.* **2004**, *126*, 6106.

[6] a) B. F. Hoskins, R. Robson, *J. Am. Chem. Soc.* **1990**, *112*, 1546; b) K. S. Min, M. P. Suh, *J. Am. Chem. Soc.* **2000**, *122*, 6834; c) O. M. Yaghi, H. Li, *J. Am. Chem. Soc.* **1996**, *118*, 295.

[7] a) M. Albrecht, M. Lutz, A. L. Spek, G. van Koten, *Nature* **2000**, *406*, 970; b) J. A. Real, E. Andrés, M. C. Muñoz, M. Julve, T. Granier, A. Bousseksou, F. Varret, *Science* **1995**, *268*, 265; c) L. G. Beauvais, M. P. Shores, J. R. Long, *J. Am. Chem. Soc.* **2000**, *122*, 2763.

[8] a) P. Horcajada, C. Serre, M. Vallet-Regí, M. Sebban, F. Taulelle, G. Férey, *Angew. Chem, Int. Ed.* **2006**, *118*, 6120; b) S. M. Cohen, *Curr. Opin. Chem. Biol.* **2007**, *11*, 115.

[9] a) O. R. Evans, W. Lin, *Chem. Mater.* **2001**, *13*, 2705; b) M. Alvaro, E. Carbonell, B. Ferrer, F. X. L. Xamena, H. Garcia, *Chem. Eur. J.* **2007**, *13*, 5106.

[10] a) N. L. Rosi, J. Eckert, M. Eddaoudi, D. T. Vodak, J. Kim, M. O'Keeffe, O. M. Yaghi, *Science* **2003**, *300*, 1127; b) A. W. C. van den Berg, C. O. Areán, *Chem. Commun.* **2008**, 668; c) D. Zhao, D. Yuan, H.-C. Zhou, *Energy Environ. Sci.* **2008**, *1*, 222.

[11] a) D. G. Kurth, M. Higuchi, *Soft Matter* **2006**, *2*, 915; b) X. Li, F. Cheng, S. Zhang, J. Chen, *J. Power Sources* **2006**, *160*, 542; c) L. Huang, H. Wang, J. Chen, Z. Wang, J. Sun, D. Zhao, Y. Yan, *Microporous Mesoporous Mater.* **2003**, *58*, 105.

[12] While this paper was in revision, several studies were published on the gas-sorption properties of coordination-polymer particles based on $\mathrm{In}^{\mathrm{III}}$ with 1,4-benzenedicarboxylate and 2,6-bis[(4-carboxyanilino)carbonyl]pyridine, respectively, as a function of their morphology: a) W. Cho, H.-J. Lee, M. Oh, *J. Am. Chem. Soc.* **2008**, *130*, 16943; b) H. J. Lee, W. Cho, S. Jung, M. Oh, *Adv. Mater.* **2009**, *21*, 674–677.

[13] a) R. N. Grimes, *Carboranes*, Academic Press, New York **1970**, p. 181; b) M. A. Surikova, N. I. Bekasova, E. A. Baryshnikova, A. A. Askadskii, V. V. Kazantseva, M. I. Busin, T. N. Kolosova, *Polym. Sci, Ser. A* **2002**, *1*, 5; c) M. F. Hawthorne, *Chem. Rev.* **1968**, *9*, 281; d) A. S. Larsen, J. D. Holbrey, F. S. Tham, C. A. Reed, *J. Am. Chem. Soc.* **2000**, *122*, 7264; e) C. A. Reed, *Chem. Commun.* **2005**, 1669; f) S. H. Lawrence, J. R. Wermer, S. K. Boocock, M. A. Banks, P. C. Keller, S. G. Shore, *Inorg. Chem.* **1986**, *25*, 367; g) M. F. Hawthorne, J. I. Zink, J. M. Skelton, M. J. Bayer, C. Liu, E. Livshits, R. Baer, D. Neuhauser, *Science.* **2004**, *303*, 1849.

[14] CCDC-682726 (**2**) and -714279 (**3**) contain the supplementary crystallographic data for this paper. These data can be obtained free of charge from The Cambridge Crystallographic Data Centre via www.ccdc.cam.ac.uk/data_request/cif.

[15] a) F. Rouquerol, J. Rouquerol, K. Sing, *Adsorption by Powders and Porous Solids. Principles, Methodology and Applications*, Academic Press, London **1999**, pp. 18–20; b) S.-I. Noro, R. Kitaura, S. Kitagawa, T. Akutagawa, T. Nakamura, *Inorg. Chem.* **2006**, *45*, 8990; c) H. Frost, T. Duren, R. Q. Snurr, *J. Phys. Chem. B* **2006**, *110*, 9565.

[16] Different solvents may also affect parameters such as pH, ionic strength and metal-cluster building-unit formation. Further studies need to be done to determine which affected parameter is the dominant contribution to the formation of a specific network.

Received: January 14, 2009
Revised: February 13, 2009